GeoConvention 2016
Calgary • Canada • March 7-11
OPTIMIZING RESOURCES

Convergence of a FWI scheme based on PSPI migration

Marcelo Guarido
CREWES – University of Calgary
Laurence R. Lines
CREWES – University of Calgary
Robert J. Ferguson
Orthogonal Geophysics

Summary (Heading in Arial 12pt bold)

A full waveform inversion (FWI) routine using PSPI migration with a deconvolution imaging condition was tested on an acoustic synthetic 2D survey using the Marmousi model. Inverted P-wave velocities obtained showed to be very close to the global minimum. The model update is computed by averaging monochromatic scaled gradients at each iteration and resulting in a high resolution inverted P velocity model. We tested different starting models to check the routine behavior and, as expected, better the initial model, better will be the migration of the residuals and the model update, resulting in higher resolution velocity inversion. The conjugate gradient was included in the routine, building more precise gradients and increasing the quality of the inverted model. Impedance inversion by trace integration was applied in the model update (gradient) showing promising results, mostly related to the inversion of thicker layers, and also presented a smoother and more continuous model, but it still requires more tests and some routine changes during this processing step.

Introduction

Seismic inversion techniques are the ones that use intrinsic informations contained in the data to determine rock properties by matching a model that "explains" the data. Some examples are the variation of amplitude per offset, or AVO (Shuey, 1985; Fatti et al., 1994), the traveltime differences between traces, named traveltime tomography (Langan et al., 1984; Bishop and Spongberg, 1984; Cutler et al., 1984), or even by matching synthetic data to the observed data, as it is done in full waveform inversion (Tarantola, 1984; Virieux and Operto, 2009; Margrave et al., 2010; Pratt et al., 1998), among others. These inversions can compute rock parameters as P and S waves velocities, density, viscosity and others. In this work we are focused in the inversion of the P wave velocity.

FWI, is a least-square based inversion, which objective is to find the model parameters that minimizes the difference between observed (acquired) data and synthetic shots (Margrave et al., 2011), or the residuals. This is accomplished in an iterative fit method by linearizing a non-linear problem.

The full waveform inversion was proposed in the early 80's (Pratt et al., 1998) but the technique was considered too expensive in computational terms. Lailly (1983) and Tarantola (1984) simplified the methodology by using the steepest-descent method (or gradient method) in the time domain to minimize the objective function without calculate, explicitly, the partial derivatives. They compute the gradient by a reverse-time migration (RTM) of the residuals. Pratt et al. (1998) develop a matrix formulation for the full waveform inversion in the frequency domain and present efficient ways to compute the gradient and the inverse of the Hessian matrix (the step length for convergence in the FWI) the Gauss-Newton or the Newton approximations. The FWI is shown to be more efficient if applied in a multi-scale method, where lower frequencies are inverted first and is increased as more iterations are done (Pratt et al., 1998; Virieux and Operto, 2009; Margrave et al., 2010). An overview of the FWI theory and studies are compiled by Virieux and Operto (2009). Lindseth (1979) showed that an impedance inversion from seismic data is not effective due to the lack of low frequencies during the acquisition but could be compensated by the match with a sonic-log profile. Margrave et al. (2010) used a gradient method and matched it with sonic logs profiles to compensate the absence of the low frequency and to calibrate the model update by computing the step length and a phase rotation (avoiding cycle skipping). They also proposed the use of a PSPI (phase-shift-plus-interpolation) migration (Ferguson and Margrave, 2005) instead of the RTM, so the iterations are done in time domain but only selected frequency bands are migrated, using a deconvolution imaging condition (Margrave et al., 2011; Wenyong et al., 2013) as a better reflectivity estimation. Warner and Guasch (2014) use the deviation of the Weiner filters of the real and estimated data as the object function with great results.

We are applying the FWI methodology using the PSPI migration Margrave et al. (2010); Ferguson and Margrave (2005) with a deconvolution imaging condition to compute the gradient. A conjugate gradient is also used to improve the quality of the gradient and to reduce the number of iterations (Zhou et al., 1995; Vigh and Starr, 2008). The step length is computed by a least-square minimization (Pica et al., 1990) and is being estimated for individual frequencies. The synthetic data is done by a finite difference forward modelling algorithm.

Theory and/or Method

The objective of the FWI methodology is to minimize an objective function. Here we minimize the residuals **$\Delta d(m)$**, that is the difference between observed data **d_0** and synthetic data **$d(m)$**, when the model **m** (here P wave velocity) is changed:

$$C(m) = \|d_0 - d(m)\|^2 = \|\Delta d(m)\|^2 \quad (1)$$

Minimizing the objective function C(m) in respect to the model m, we can to the steepest-descent formula (Pratt et al.,1998):

$$m_{n+1} = m_n + \alpha_n g_n \quad (2)$$

where **α** is the step length, **g** is the gradient and **n** is the n-th iteration. This equation shows that a model update can be obtained by adding a scaled gradient to the actual model. This routine is kept until stp criteria I reached. The gradient is computed by a reverse time migration of the residuals (Tarantola, 1984; Pratt et al., 1998; Virieux and Operto, 2009) but we decided to use the phase-shift-plus-interpolation (PSPI) migration. Usually the FWI routine is to start by updating the model using low frequencies and after update higher frequencies. We follow the same strategy. For each iteration we start with a range of low frequencies (2-4Hz) and increase the range by 2Hz (2-6Hz and so on) when convergence is reached. For each iteration we migrate unique frequencies of the residuals and obtain a monochromatic gradient. We then compute the step length for each frequency and average the scaled gradients as the model update, leading equation 2 to:

$$m_{n+1} = m_n + \frac{1}{N}\sum_{i=1}^{N} \alpha_n(\omega_i) g_n(\omega_i) \quad (3)$$

The step length is computed using Pica et al. (1990) algorithm:

$$\alpha_n = \frac{[F_n g_n]^T [d_0 - d(m_n)]}{[F_n g_n]^T [F_n g_n]} \quad (4)$$

where the term **$F_n g_n$** is a finite difference operator around a perturbation **ε** of the model **m_n**. This only one forward modelling.

Later we replace the gradient **g_n** on equation 3 by the conjugate gradient **h_n** (Zhou et al., 1995; Vigh and Starr, 2008; Ma et al., 2010):

$$m_{n+1} = m_n + \alpha_n h_n \quad (5)$$

where

$$h_0 = g_0, \quad \beta_n = \frac{{g_n}^T(g_n - g_{n-1})}{{g_{n-1}}^T g_{n-1}}, \quad h_n = g_n + \beta_n h_{n-1} \tag{6}$$

The gradient is a migrated result: reflection coefficients. We apply an impedance inversion by assuming constant density and small contrasts in velocity (Treitel et al., 1995), leading to the exponential form:

$$V(t) = V_0 e^{2\int_{t_1}^{\tau} R(\tau)d\tau} \tag{7}$$

Examples

Tests are done on synthetic data using the Marmousi model of figure 1. The survey has 105 shots, 100m spacing, with 601 receivers in a split-spread geometry and 10m spacing. The forward modeling is done using an acoustic finite difference algorithm with a Ricker wavelet of 5Hz dominant frequency.

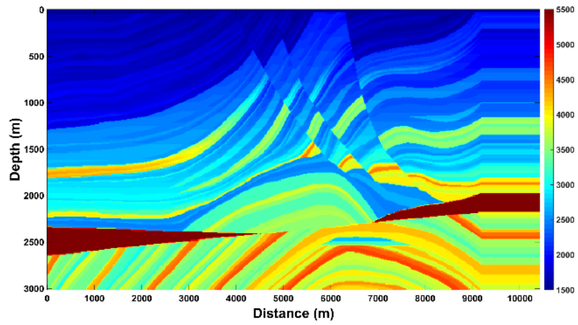

Figure 1: The Marmousi acoustic model used for the tests.

Figure 2 shows the resulting invertion by using the classic gradient (non-conjugate) with different initial models. We show that better is the starting model, more precise is the resulting inverted model. This can be explained as the migrated residuals have the migrated reflectors on a more correct position when the migration velocity is better and the model update is improved.

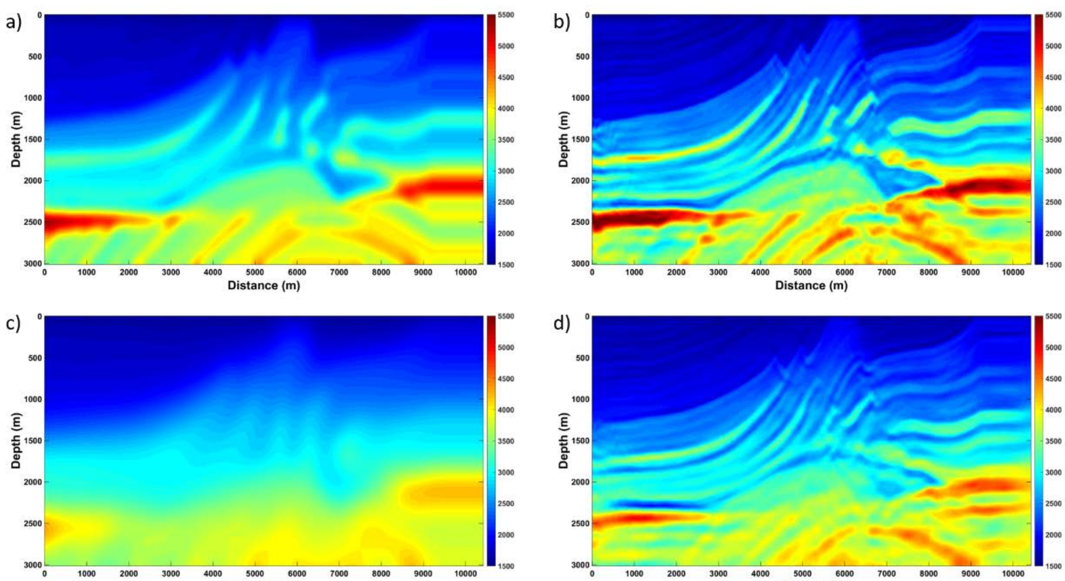

Figure 2: a) and c) are the initial models and b) and d) are the respectivity inverted model. The quality of the inversion is improved when the starting model is closer to the real one.

When the conjugate gradient of the equation 6 is used, the inverted model has an improved quality and is closer to the real one, using the starting model same as used for the classic gradient (figure 3).

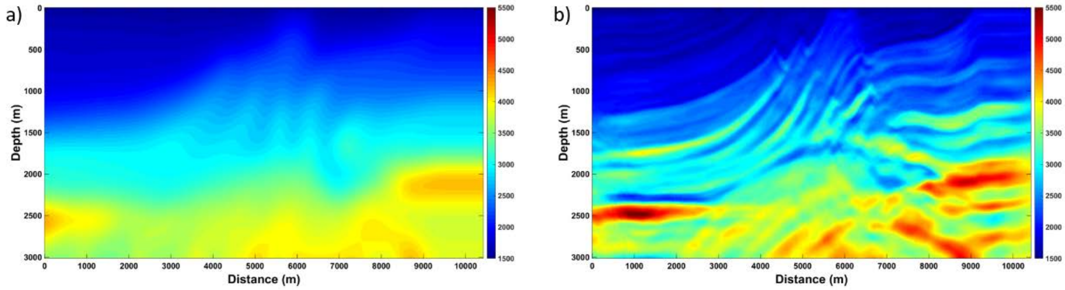

Figure 3: a) is the initial model and b) is the improved conjugate gradient invertion.

Finally, figure 4 shows the inverted model when an impedance inversion is applied trace by trace of the gradient (reflection coefficients). The result is promising and looks more continuous than the others inversions but more tests are required and it is subject for future work.

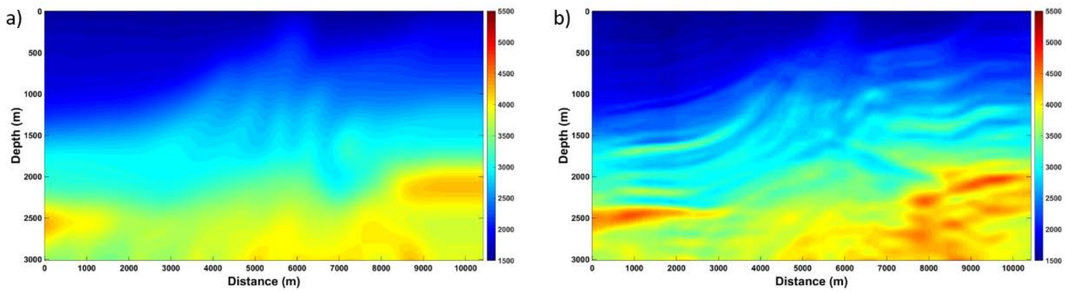

Figure 4: a) is the initial model and b) inverted model when an impedance inversion is applied.

Conclusions

Applying a full waveform inversion scheme based on PSPI migration shows great results on acoustic synthetic data. The routine is fast and stable and allows us to apply it on time domain but select only desired frequncies to migrate the residuals. We could obtain better results when lower frequencies are inverted first and higher frequncies later.

We compute an averaged gradient based on monochromatic scale gradients for each iteration and the inverted models have higher resolution even with no impedance inversion (using only reflection coefficients to update the model). Better results are reached when the starting model is closer to the real one. Mostly due to the better migrated residuals when a better migration velocity is used.

The conjugate gradient improved the routine leading to a inverted model closer to the global minimum (the real model) using the same initial model on the classic gradient inversion.

Impedance inversion of the gradient is looks like to be a good strategy to update the model, as the gradient is better converted to reflection coefficients to impedance. We obtained promising results but it is still unstable and more tests are required. This is a subject for future work.

Acknowledgements

The authors thank the sponsors of CREWES for continued support. This work was funded by CREWES industrial sponsors and NSERC (Natural Science and Engineering Research Council of Canada) through the grant CRDPJ 461179-13. We thank Gary Margrave and Soane Mota dos Santos for the suggestions, tips and productive discussions, and Babatunde Arenrin for providing the step length estimation code.

References

Bishop, T. N., and Spongberg, M. E., 1984, Seismic tomography: A case study: SEG Technical Program Expanded Abstracts, 313, 712–713.

Cutler, R. T., Bishop, T. N., Wyld, H. W., Shuey, R. T., Kroeger, R. A., Jones, R. C., and Rathbun, M. L., 1984, Seismic tomography: Formulation and methodology: SEG Technical Program Expanded Abstracts, 312, 711–712.

Fatti, J. L., Smith, G. C., Vail, P. J., Strauss, P. J., and Levitt, P. R., 1994, Detection of gas in sandstone reservoirs using avo analysis: A 3-d seismic case history using the geostack technique: Geophysics, 59, No. 9, 1362–1376.

Ferguson, R., and Margrave, G., 2005, Planned seismic imaging using explicit one-way operators: Geophysics, 70, No. 5, S101–S109.

Guarido, M., Lines, L., and Ferguson, R., 2014, Full waveform inversion - a synthetic test using the pspi migration: CREWES Research Report, 26, 26.1–26.23.

Guarido, M., Lines, L., and Ferguson, R., 2015, Full waveform inversion: a synthetic test using pspi migration: SEG Technical Program Expanded Abstract, 279, 1456–1460.

Lailly, P., 1983, The seismic inverse problem as a sequence of before stack migrations: Conference on inverse scattering, theory and application: Society of Industrial and Applied Mathematics, Expanded Abstracts, 206–220.

Langan, R. T., Lerche, I., Cutler, R. T., Bishop, T. N., and Spera, N. J., 1984, Seismic tomography: The accurate and efficient tracing of rays through heterogeneous media: SEG Technical Program Expanded Abstracts, 314, 713–715.

Lindseth, R. O., 1979, Synthetic sonic logs-a process for stratigraphic interpretation: Geophysics, 44, No. 1, 3–26.

Ma, Y., Hale, D., Meng, Z. J., and Gong, B., 2010, Full waveform inversion with image-guided gradient: SEG Technical Program Expanded Abstracts, 198, 1003–1007.

Margrave, G., Ferguson, R., and Hogan, C., 2010, Full waveform inversion with wave equation migration and well control: CREWES Research Report, 22, 63.1–63.20.

Margrave, G., Yedlin, M., and Innanen, K., 2011, Full waveform inversion and the inverse hessian: CREWES Research Report, 23, 77.1–77.13.

Pica, A., Diet, J. P., and Tarantola, A., 1990, Nonlinear inversion of seismic reflection data in a laterally invariant medium: Geophysics, 55, No. 2, R59–R80.

Pratt, R. G., Shin, C., and Hick, G. J., 1998, Gauss-newton and full newton methods in frequency-space seismic waveform inversion: Geophysical Journal International, 133, No. 2, 341–362.

Shuey, R. T., 1985, A simplification of the zoeppritz equations: Geophysics, 50, No. 4, 609–614.

Tarantola, A., 1984, Inversion of seismic reflection data in the acoustic approximation: Geophysics, 49, No. 8, 1259–1266.

Treitel, S., Lines, L., and Ruckgaber, G., 1995, Seismic impedance estimation: Geophysical Inversion and Applications - Memorial University of Newfoundland, 1, 6–11.

Vigh, D., and Starr, E.W., 2008, 3d prestack plane-wave, full-waveform inversion: GEOPHYSICS, 73, No. 5, VE135–VE144.

Virieux, J., and Operto, S., 2009, An overview of full-waveform inversion in exploration geophysics: Geophysics, 74, No. 6, WCC1–WCC26.

Warner, M., and Guasch, L., 2014, Adaptive waveform inversion: Theory: SEG Technical Program Expanded Abstracts, 207, 1089–1093.

Wenyong, P., Margrave, G., and Innanen, K., 2013, On the role of the deconvolution imaging condition in full waveform inversion: CREWES Research Report, 25, 72.1–72.19.

Zhou, C., Cai, W., Luo, Y., Schuster, G. T., and Hassanzadeh, S., 1995, Acoustic wave-equation traveltime and waveform inversion of crosshole seismic data: GEOPHYSICS, 60, No. 3, 765–773.